Imaging and Radiation Research 2024, 7(1), 4085.
https://doi.org/10.24294/irr.v7i1.4085

Article

Generation of PAS-stained images of glomerular tissue units using a generative adversarial network with spectral normalization colorization method

Jincheng Peng, Guoyue Chen*, Kazuki Saruta, Yuki Terata

Department of Information and Computer Science, Akita Prefectural University, Akita Yurihonjo 015-0055, Japan
*** Corresponding author:** Guoyue Chen, chen@akita-pu.ac.jp

CITATION

Peng J, Chen G, Saruta K, Terata Y. Generation of PAS-stained images of glomerular tissue units using a generative adversarial network with spectral normalization colorization method. Imaging and Radiation Research. 2024; 7(1): 4085. https://doi.org/10.24294/irr.v7i1.4085

ARTICLE INFO

Received: 27 November 2023
Accepted: 5 February 2024
Available online: 7 March 2024

Abstract: In recent years, the pathological diagnosis of glomerular diseases typically involves the study of glomerular his-to pathology by specialized pathologists, who analyze tissue sections stained with Periodic Acid-Schiff (PAS) to assess tissue and cellular abnormalities. In recent years, the rapid development of generative adversarial networks composed of generators and discriminators has led to further developments in image colorization tasks. In this paper, we present a generative adversarial network by Spectral Normalization colorization designed for color restoration of grayscale images depicting glomerular cell tissue elements. The network consists of two structures: the generator and the discriminator. The generator incorporates a U-shaped decoder and encoder network to extract feature information from input images, extract features from Lab color space images, and predict color distribution. The discriminator network is responsible for optimizing the generated colorized images by comparing them with real stained images. On the Human Biomolecular Atlas Program (HubMAP)—Hacking the Kidney FTU segmentation challenge dataset, we achieved a peak signal-to-noise ratio of 29.802 dB, along with high structural similarity results as other colorization methods. This colorization method offers an approach to add color to grayscale images of glomerular cell tissue units. It facilitates the observation of physiological information in pathological images by doctors and patients, enabling better pathological-assisted diagnosis of certain kidney diseases.

Keywords: spectral normalization; generative adversarial networks; PAS staining; medical image colorization

1. Introduction

Stained tissue unit: The three-dimensional cellular cluster with the glomerular capillaries at its center constitutes the functional tissue unit (FTU) of the renal glomerulus. Pathologists have studied FTU stained sections to analyze a number of common renal diseases [1]. These tissue units are collected and analyzed by pathology experts during biopsy, often employing Periodic Acid-Schiff stain (PAS) for staining [2]. The PAS-stained whole tissue units are subsequently scanned under an electron microscope to generate stained tissue unit et al. slice images corresponding to relevant areas. In this process, based on the images post-staining, an evaluation of the diffusion distance between each cell and other cells within the entire tissue scan is conducted to analyze the pathological causes of kidney diseases. However, the manual staining of FTU slices is exceedingly intricate, necessitating the utilization of chemical reagents by specialized staining pathologists to color the tissue cells, This approach is characterized by lengthy staining cycles, high costs, and the potential irreversible

damage to tissue caused by the employed chemical reagents, Moreover, the inconsistency in the depth of staining for pathological slice sections diminishes the reusability of the slices, These challenges call for computer image digitization as a solution. Because of the deep learning has made amazing advances in the field of computer vision in recent years, the mainstream approach to image colorization is no longer traditional machine learning. Instead, it uses the powerful parametric learning capabilities of deep neural networks to learn how to select, propagate and predict color distributions from large-scale data.

Iizuka et al. [3] converted the image colorization problem into an image classification task, utilizing a two-channel network that combines local feature information and global prior knowledge in images to achieve automatic colorization of grayscale images of arbitrary sizes. However, this network solely employed convolutional neural networks for predicting color distributions, leading to a loss of pixel semantic information, resulting in misclassification and unnatural colorization compared to the original images. Zhang et al. [4] addressed this limitation by stacking multiple convolutional layers to predict the probabilities of 313 ab color channels in the Lab color space, thereby effectively predicting the color distribution of the dataset. Larsson et al. [5] integrated a VGG neural network for semantic parsing and localized information extraction into the colorization system. This system predicts color histograms for each image location to anticipate color distributions for individual pixels. While these methods exhibited further improvements in colorization effects, they still struggle to resolve issues such as desaturated generated images, yellowish tones, unnatural colorization, and the susceptibility to gradient vanishing during training.

Over the past few years, with the rapid development of generative adversarial network, the field of automatic image colorization as a branch of image restoration has witnessed significant advancements, garnering consistent attention from researchers. The literature [6] proposes a method for image colorization by using deep convolutional generative adversarial network, This method uses a discriminator to predict the loss of the generated image from the real image to predict the color distribution of each pixel. Cao et al. [7] utilized an unsupervised colorization network based on cGAN for image colorization, where the generator was designed without an encoder-decoder structure. Instead, it incorporated random optimization noise at various layers of fully convolutional layers, this approach enhanced realism and diversified image generation, yet the increased noise introduction led to uncontrollable randomness and compromised colorization quality. To address the instability of Generative Adversarial Networks (GANs), a method was proposed in the study by Miyato et al. [8] that replaces the original normalization structure with spectral normalization. This ensures that the discriminator D satisfies Lipschitz continuity, restricting the degree of drastic changes in the function. As a result, this stabilizes the GAN model and makes it more robust.

Early studies on traditional medical image colorization relied on transferring false-color information from real objects to medical image datasets, highlighting subtle details that were hard to discern. A method proposed by Lagachinski et al. [9] employed user annotations and mixed distance transformations for medical image

colorization, However, this method was based on manual coloring of specified regions, falling short of complete automation. In 2016, Khan et al. [10] presented a method to migrate colors from endoscopic images to grayscale endoscopic images, This approach generated physical colors based on dictionary-based color mapping, which were then applied to preprocessed grayscale images to reproduce colors. However, this method utilized shallow handcrafted feature extraction, resulting in less satisfactory colorization, slow efficiency, and the risk of information loss. Liang et al. [11] propose a colorization network based on the Cycle Generative Adversarial Network (CycleGAN) model, applying style transfer to the coloring of medical images. In 2023, Chen [12] propose a self-supervised coloring framework based on Cycle Generative Adversarial Network (CycleGAN), treating the coloring of medical images as a cross-modal domain transfer problem in the color space.

Building on the previous discussion regarding the colorization of medical images using Generative Adversarial Networks (GANs) and the research on spectral normalization. In this paper, we propose an automatic colorization method based on spectral normalization generative adversarial networks for color recovery of gray-scale images of glomerular tissue unit, The network is divided into two structures, the generator and the discriminator, the generator is used to extract the feature information of the image, and the general feature information of the image is obtained by generative network block, The U-shaped decoder and encoder network is introduced in the generator, which extracts the original L-channel grayscale image features and predicts the color distribution of the ab channel by skipping connections, The network of discriminators is responsible for optimizing the combined chromatic map to obtain the final color image. This method utilizes a generative adversarial network to generate new colorized images, enhancing the naturalness, saturation, and realism of the resulting images, which closely resemble actual PAS-stained images of glomerular cell tissue units. Moreover, the discriminator of the GAN introduces a spectral normalization module to replace the original normalization module, enhancing the GAN's stability by ensuring the discriminator satisfies Lipschitz continuity. Finally, an evaluation of colorization structure was performed on both glomerular tissue unit-stained images and the original PAS-stained images using peak signal-to-noise ratio and structural similarity indices. On the Human BioMolecular Atlas Program (HuBMAP)—Hacking the Kidney FTU segmentation challenge dataset, we achieved a peak signal-to-noise ratio of 29.802 dB, along with high structural similarity results. As the PAS-stained images of glomerular tissue units involve predicting a simplified color category distribution, the predicted colorized images closely resemble the actual original PAS-stained tissue images. Hence, this method holds significant practical and research value. The colorized images can aid in the pathological diagnosis of certain kidney diseases.

2. Methods

In this chapter we describe in detail the structure of spectral normalized generative adversarial colorization networks.

2.1. Network structure

The entire network structure is shown in **Figure 1**. The spectral normalization generative adversarial network model consists of two parts: the generator and the discriminator, At the same time, spectral normalization was added to the discriminator to improve the normalization method used before. In this paper, the Lab color space is used for color prediction, The grayscale image of the L channel component is passed through a generator to predict the a and b chrominance channel components. $X_l \rightarrow \widetilde{X_{ab}}$. The generated $\widetilde{X_{ab}}$ component is combined with the original L-channel to form a colorized image, which serves as the input image for the discriminator. The discriminator network discriminates and distinguishes between the input virtual colorized image and the real color image until it can no longer differentiate them, producing an infinitely close approximation of the real colorized image. This can predict the color distribution of the original cellular tissue grayscale image. Finally, a PAS-stained image of the glomerular tissue unit that closely resembles reality is generated.

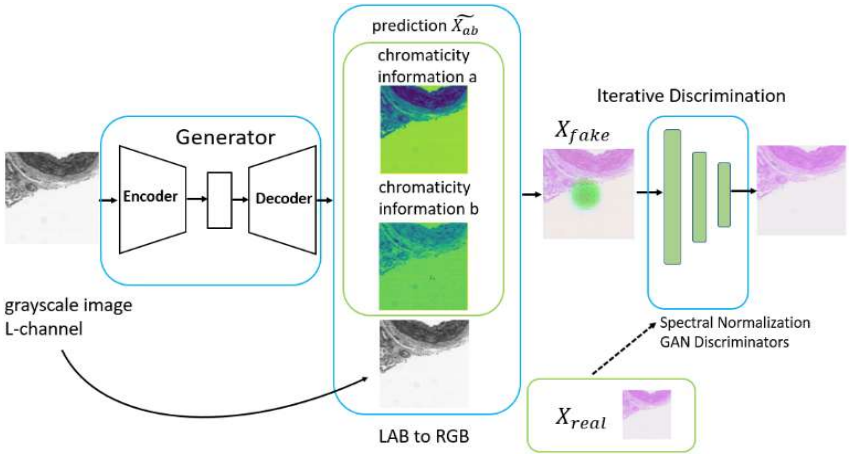

Figure 1. The spectral normalization generative adversarial network structure.

2.2. Generative network block

The generator network employs a U-shaped architecture consisting of an encoder and a decoder, as illustrated in **Figure 2**. The architecture includes downsampling convolutional modules, a bridging module, and upsampling convolutional modules [13]. The network takes grayscale images of glomerular tissue units in the Lab color space as input, specifically the luminance information from the L channel. The output comprises chromatic information (ab) for the PAS-stained images of glomerular tissue units. The left side represents the encoder, comprising 7 downsampling modules. Each downsampling module consists of a convolutional layer (with a 4 × 4 kernel size), normalization layer, and LeakyReLU layer. The downsampling convolutional modules are responsible for extracting feature structures from the images, progressively capturing high-level semantic information and color texture details. The right side corresponds to the decoder, composed of 7 upsampling modules. Each upsampling module includes a deconvolutional layer (with a 4 × 4 kernel size), normalization layer, and LeakyReLU layer. The downsampling modules serve to consolidate the encoded image information for reconstruction and precision. The

output from each block in the encoding area is connected to its corresponding block in the decoding area through skip connections. These skip connections facilitate the direct transfer of shallow-level information to the same-height deconvolutional layers, resulting in images with reasonably consistent overall colorization.

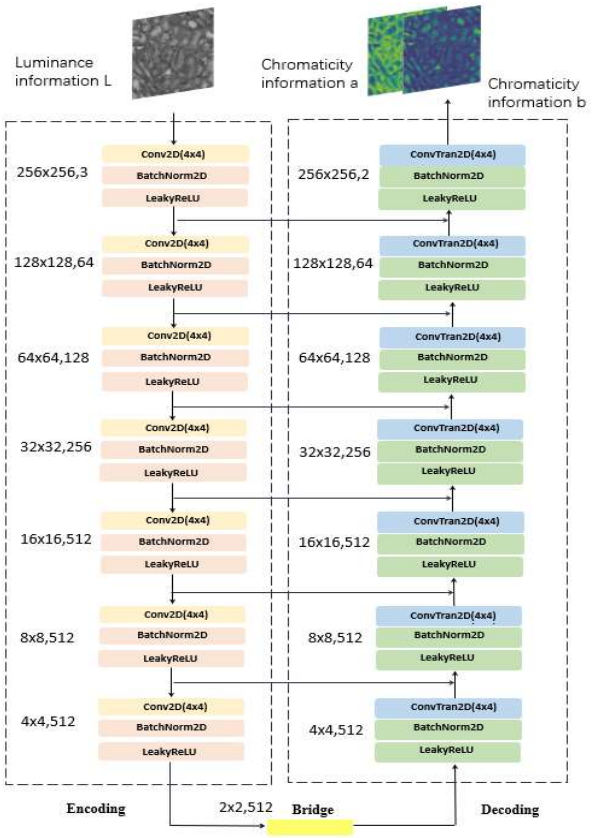

Figure 2. Generative network block structure.

2.3. Discriminator network block

The discriminator in this paper, as shown in **Figure 3**, uses a typical discriminator in a conditional generative adversarial network, with spectral normalization replacing the normalization module in each layer. The discriminator in the conditional generative adversarial network introduces domain information and applies constraints to control the content generated by the network, transforming an unsupervised network into a supervised model. By introducing a reference image as input condition to the discriminator, the color information of the target generated image is supervised to obtain colors that are consistent with the reference image. The network structure of the discriminator is shown in **Figure 3**, which includes four convolutional layers with a kernel size of 4 × 4. The first three layers have a convolution stride of 2 to obtain a larger receptive field, and the last layer has a stride size of 1 [14]. Finally, a fully connected (FC) layer is used to integrate and classify feature information. For an input image with a resolution of 256 × 256, the generated color is compared with the reference image to produce colors that are more consistent with the reference image.

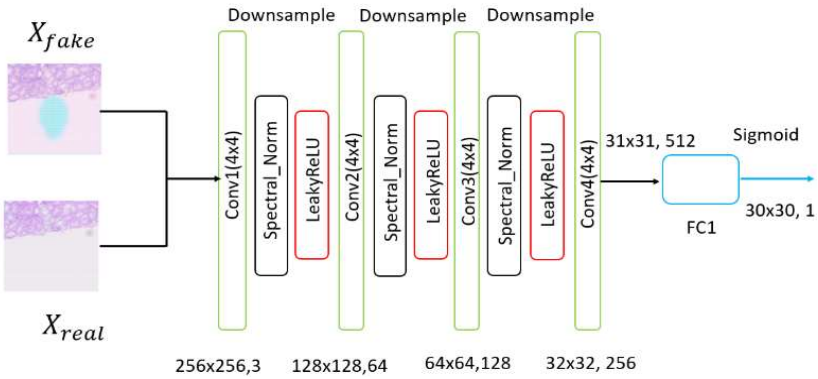

Figure 3. Discriminator network block structure.

2.4. Spectral normalization

There are problems with gradient disappearance and pattern collapse in generative adversarial networks, which are related to the mechanisms of generative adversarial networks. The generative adversarial network suffers from Kullback-Leibler (KL) dispersion asymmetry, which makes the generative adversarial network obsessed with the accuracy of the discriminator, thus ignoring the diversity of generator generation patterns. resulting in the patterns learned by the generator covering only some of the patterns in the real data, making the diversity of the generated samples low and eventually leading to a pattern collapse in the model.

The spectral normalization structure normalizes the weights of each layer in a neural network based on their spectral norms, this is achieved by performing singular value decomposition on the weight matrices and then constraining the singular values within a predefined range, thereby calculating and controlling the spectral norm of the weight matrix [8]. In contrast to some complex normalization techniques, spectral normalization incurs low computational costs, requires no additional hyperparameter tuning, enhances training stability, and effectively addresses the aforementioned issues. Spectral normalization is defined as:

$$W_s(W) := \frac{W}{\sigma(W)} \tag{1}$$

W is the parameter matrix that is subjected to normalization to control the spectral norm, W_s is Spectral Normalized Weight Matrix, σ is Spectral Normalization Singular Value**,** the spectral normalization makes the discriminant network satisfy the lipschitz constraint, where K is the maximum singular value of the matrix W:

$$\sigma(W_s(W)) := \sigma\left(\frac{W}{\sigma(W)}\right) = \frac{1}{K}\sigma(W) = 1 \tag{2}$$

It is thus demonstrated that adding spectral normalization to the network can make the discriminator network satisfy the condition that the Lipschitz, constant Lipschitz is equal to 1 by strictly constraining the spectral norm of the weight matrix of each network layer ,and without destroying the structure of the weight matrix, thus enhancing the stability of the deep convolutional generative adversarial network in training and improving the generator performance of the deep convolutional generative adversarial network and the discriminator performance of the discriminator.

2.5. Loss function

In this paper, the design of the loss function is divided into two parts, which are the generator loss function and the discriminator loss function. where the loss function L1 of the distance between the generated image and the target image is defined using the MAE [15] (mean-absolute error) loss function. The mean absolute error loss function calculates the mean absolute error of the images generated by each color channel in the generator with respect to the standard stained slices in the input discriminator network, where the MAE is expressed as follows:

$$MAE = \frac{1}{MN}\sum_{p=0}^{M-1}\sum_{q=0}^{N-1}\left|z_{\text{label}}(p,q) - z_{\text{output}}(p,q)\right| \tag{3}$$

M represents the number of rows in a matrix or the size of the first dimension, N represents the number of columns in a matrix or the size of the second dimension, p is a variable used to denote the row index in the pixels, q is a variable used to denote the column index in the pixels, z_{label} is translated as reference color image, z_{output} is translated as predicted color image.

The discriminator loss for the generating adversarial colorization model is described as:

$$L_D = E_{x\sim P_{data}}[logD(x,C,y)] + E_{x\sim P_{data}}[\log(1 - D(x,C,G(x,C))] \tag{4}$$

Its generator loss is described as:

$$L_G = E_{x\sim P_{data}}[\log(1 - D(x,C,G(x,C))] + L_1 \tag{5}$$

where $D(*)$ denotes the discriminator, $G(*)$ denotes the generator, x denotes the gray target image, C denotes the feature condition of the reference image, and y denotes the original color information of the image.

2.6. Evaluation method

Due to the uncertainty of the colorization task, the general mainstream evaluation method uses the peak signal-to-noise ratio and structural similarity metrics in the image restoration task to evaluate the quality of the images generated by the coloring algorithm. peak signal-to-noise ratio (PSNR) is the ratio between the maximum possible signal power and the destructive noise power which affects its accuracy. The maximum signal-to-noise ratio is often expressed in logarithmic decibels. PSNR was defined as Mean Square Error (MSE). For the generated colorization images with standard colorization images, if one is an approximation of another's noise, the PSNR between them is defined as:

$$PSNR = 10\,log_{10}(\frac{MAX^2}{MSE}) \tag{6}$$

MAX represents the maximum possible pixel value in the image.

Structural similarity [16] (SSIM) is often used as an indicator to assess image quality, generally measuring the similarity of two images in terms of contrast, brightness and resulting information. In this paper, structural similarity is used to compare the similarity between the generated stained images and the real colorization images, and the larger the structural similarity value, the closer the two images are, the better the learning effect. structural similarity can be defined as:

$$SSIM(X,Y) = \frac{(2\mu_X\mu_Y + c_1)(2\sigma_{XY} + c_2)}{(\mu_X^2 + \mu_Y^2 + c_1)(\sigma_X^2 + \sigma_Y^2 + c_2)} \quad (7)$$

where μ_x is the mean of X, μ_y is the mean of image Y, σ_x^2 is the covariance of X, σ_y^2 and similarly is the covariance of Y, σ_{XY} representing the covariance of X and Y, c_1 and c_2 are constants that maintain stability.

3. Experiments

3.1. Database

HuBMAP - Hacking the Kidney FTU segmentation challenge dataset [11,17] was used to evaluate our model. This dataset, published by the HuBMAP organization, includes 11 fresh frozen and 9 formalin-fixed paraffin embedded PAS kidney tissue samples. Each sample includes PAS stained FTU images and annotation labels, with 8 training sets and 5 public test sets, consisting of TIFF files. To prepare the data, we sliced out 9580 PAS colorization images with FTU annotation labels from the TIFF files. As we only needed the original tinted image without annotation labels, we cropped the images to 256 × 256 as the original size was too large and would have wasted storage space.

Furthermore, we converted the color space from RGB to Lab, and extracted the L luminance channel information as the network input image. The information on the luminance channels a and b were used as the target image. The data processing steps is shown in **Figure 4**.

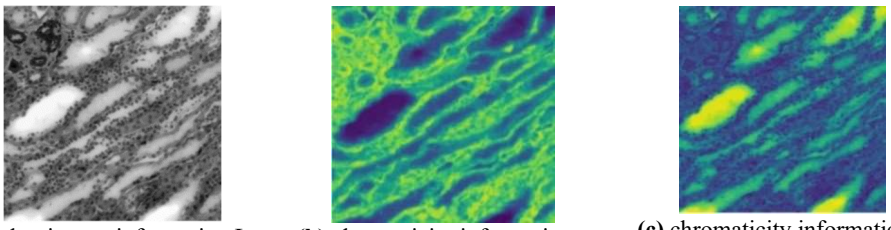

(a) luminance information L **(b)** chromaticity information a **(c)** chromaticity information b

Figure 4. Lab color space pre-processing of Kidney FTU segmentation challenge dataset.

3.2. Implementation details

All training and testing experiments are performed on workstations. The CPU used is Intel (R) Xeon (R) CPU e52630V4@2,20GHz. The GPU uses two NVIDIA forcedx1080ti with 12GB GPU memory, with a total memory of 24 G. All network architectures are implemented with pytorch 1.7.1+cu101 framework. We start the training with a batch size of 10. The proposed architecture is optimized by the Adam optimizer with the learning rate initially set to 0.0001, β_1 = 0.5, β_2 = 0.999, The loss function is used as the combined loss function mentioned earlier.

3.3. Comparisons with other method

Table 1 shows the PSNR and SSIM assessment results from the table below. It can be seen that the generated adversarial network model with spectral normalization has the highest average PSNR score after comparing with other coloring networks,

which is 1.193 dB higher than the DCGAN model with only normalized structure. From **Figure 5**, it can be seen that the Colorful Image Colorization coloring network proposed by Zhang [3] in the ECCV2016 conference has a low distribution of color prediction, and the overall coloring effect is purple. The real tissue stained cells are light pink, and the background area that was originally white was also predicted to be purple. The subsequently proposed method, Real-Time User-Guided Image Colorization with Learned Deep Priors, has improved the metrics of PSNR and SSIM, but there is still a gap between the staining effect and the color prediction of real tissue-stained cells. The AutoEncoder coloring method is slightly higher than the generative adversarial network in terms of structural similarity values, though. However, the color was misclassified in the circle region as in the fourth figure of **Figure 5**, and the original prediction of black classification was colored by the network with mauve, while the latter two groups were predicted to be black classification using the generative adversarial network.

Table 1. Different colorization methods peak signal-to-noise ratio a structural similarity on the Kidney FTU segmentation challenge dataset.

Methods	Zhang	Real-Time	Autoencoder	Dcgan	Our
PSNR	25.656	25.689	26.862	28.609	29.802
SSIM	0.839	0.855	0.867	0.866	0.911

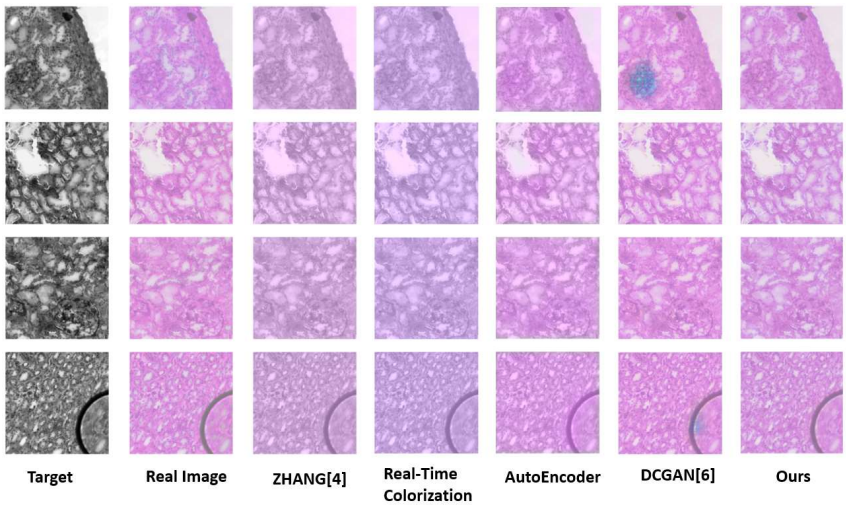

Figure 5. Different colorization methods effect on the Kidney FTU segmentation challenge dataset.

This shows that the generative adversarial network approach can generate sufficiently realistic images to deceive the discriminant through the generator, this method can better learn the image color distribution model, so that the colorization image is closer to the actual natural colorization. From the last two sets of colorization results, it can be seen that deep convolutional generative adversarial network (GANs) perform poorly on images in the test dataset that differ significantly from the training distribution. This is evidenced by the appearance of blotchy, uncolored blue spots, which lead to a decrease in PSNR. In contrast, the GAN-based colorization network

with the added spectral normalization structure did not produce these blotchy, uncolored spots. Overall, the PSNR table indicates that the improved spectral normalization GAN-based colorization model proposed in this study generates images with higher quality and better resemblance to the original stained images. This improves the overall level of image colorization and can help standardize it as a routine staining practice.

We also tested the structural similarity loss of DCGAN and SN-DCGAN, the structural similarity loss values from the similarity curves in **Figure 6** demonstrate that, with the incorporation of spectral normalization, the structural similarity values are higher than those of the deep convolutional generative adversarial network (DCGAN) model. After 40 epochs of training, structural similarity values continue to increase as the number of training batches rises. This observation provides evidence that integrating spectral normalization can enhance the color prediction capability of the deep convolutional generative adversarial network model, resulting in improved colorization outcomes.

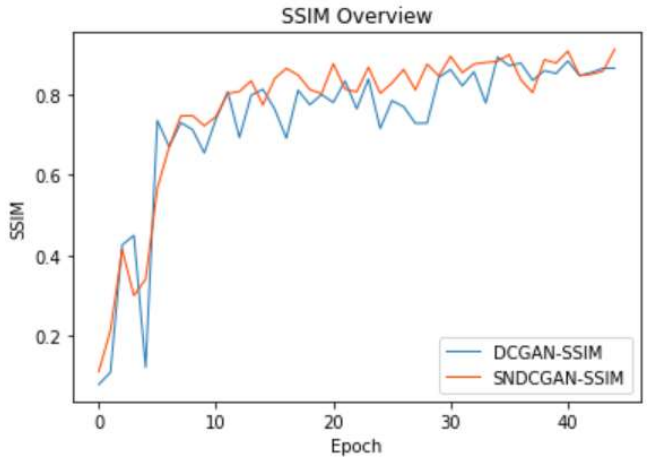

Figure 6. Structural similarity for DCGAN, SNDCGAN (Spectral Normalized DCGAN).

4. Discussion

This study applies a generative adversarial network by Spectral Normalization colorization method for PAS stained images of Glomerular Tissue Unit. improving upon the disorganized blue and uncolored spots generated by DCGAN. The enhancements aim to make the final generated color images more closely resemble the original stained images. It has been validated that Spectrum Normalization DCGAN (SN-DCGAN) achieves improved coloring results. However, there are certain limitations to this study. The experiments are confined to pseudo-coloring grayscale images, and despite the good coloring results achieved, there is still a gap compared to real stained images. The research also does not delve into how to control implicit features to control the diversity of coloring samples. Future research will focus on addressing these limitations through model and method improvements.

5. Conclusion and future works

In many cases, the diagnosis and treatment of various kidney diseases require assistance from pathological staining and slicing. However, the production of pathological staining slides in clinical practice involves a complex process. The current PAS staining slide production technique is time-consuming, labor-intensive, and may pose challenges in terms of staining. In this paper, we propose an automatic coloring method using a spectral normalization Generative Adversarial Network (GAN) to restore color to grayscale images of glomerular tissue units. This method has the advantage of generating more natural and saturated coloring effects, closely resembling the appearance of real glomerular tissue unit PAS staining images. Additionally, the discriminator of the Generative Adversarial Network includes a spectral normalization module, replacing the traditional normalization module. This ensures that the discriminator D satisfies Lipschitz continuity, thereby restricting the intensity of variations in the Generative Adversarial Network. We tested and trained our model on the HuBMAP—Hacking the Kidney glomerular functional tissue unit FTU cGAN segmentation challenge dataset. The experiments demonstrate that the color images generated by the Generative Adversarial Network are clear, natural, and closely resemble the original glomerular tissue unit staining images. It can be used for the diagnosis and analysis of kidney diseases. However, there is still a gap when directly applying this algorithm to the large-scale clinical application of staining and slicing PAS unstained images due to differences, such as contrast, in the grayscale images and unstained images used for training in this paper. Future research should focus on the registration of unstained images and real stained images to address this issue. It is also expected to be extended to general monochrome tissue and cell slicing staining methods, contributing to large-scale and random pathological staining slice clinical studies.

Author contributions: Conceptualization, JP and GC; methodology, JP and GC; software, JP; validation, JP and GC; investigation, JP; resources, GC; data curation, JP; writing—original draft preparation, JP; writing—review and editing, JP; visualization, JP; supervision, GC, KS and YT; project administration, GC; funding acquisition, GC. All authors have read and agreed to the published version of the manuscript.

Acknowledgments: This work is supported in part by JSPS KAKENHI Grant Number 23K02635.

Conflict of interest: The authors declare no conflict of interest.

References

1. Schell C, Wanner N, Huber TB. Glomerular development – Shaping the multi-cellular filtration unit. Seminars in Cell & Developmental Biology. 2014; 36: 39-49. doi: 10.1016/j.semcdb.2014.07.016
2. Yang S, Wang J, Chen Y, et al. Concurrent Kidney Glomerular and Interstitial Lesions Associated with Kimura's Disease. Nephron. 2019; 143(2): 92-99. doi: 10.1159/000501638
3. Iizuka S, Simo-Serra E, Ishikawa H. Let there be color! ACM Transactions on Graphics. 2016; 35(4): 1-11. doi: 10.1145/2897824.2925974

4. Zhang R, Isola P, Efros AA. Colorful image colorization. In: Leibe B, Matas J, Sebe N, Welling M (editors). *Computer Vision—ECCV 2016*, Proceedings of 14th European Conference; 11–14 October 2016; Amsterdam, The Netherlands. Springer; 2016. pp. 649–666. doi: 10.1007/978-3-319-46487-9_40
5. Larsson G, Maire M, Shakhnarovich G. Learning representations for automatic colorization. In: Leibe B, Matas J, Sebe N, Welling M (editors). *Computer Vision—ECCV 2016*, Proceedings of 14th European Conference; 11–14 October 2016; Amsterdam, The Netherlands. Springer; 2016. pp. 577–593. doi: 10.1007/978-3-319-46493-0_35
6. Nazeri K, Ng E, Ebrahimi M. Image colorization using generative adversarial networks. In: Perales FJ, Kittler J (editors). *Articulated Motion and Deformable Objectives*, Proceedings of 10th International Conference, AMDO 2018; 12–13 July 2018; Palma de Mallorca, Spain. Springer, Cham; 2018. pp. 85–94. doi: 10.1007/978-3-319-94544-6_9
7. Cao Y, Zhou Z, Zhang W, Yu Y. Unsupervised diverse colorization via generative adversarial networks. In: Ceci M, Hollmén J, Todorovski L, et al. (editors). *Machine Learning and Knowledge Discovery in Databases*, Proceedings of European Conference, ECML PKDD 2017; 18–22 September 2017; Skopje, Macedonia. Springer, Cham; 2017. pp. 151–166. doi: 10.1007/978-3-319-71249-9_10
8. Miyato T, Kataoka T, Koyama M, et al. Spectral normalization for generative adversarial networks. ArXiv. 2018.
9. Lagodzinski P, Smolka B. Colorization of medical images. Asia-Pacific Signal and Information Processing Association; 2009.
10. Khan TH, Mohammed SK, Imtiaz MS, et al. Efficient Color Reproduction Algorithm for Endoscopic Images Based on Dynamic Color Map. Journal of Medical and Biological Engineering. 2016; 36(2): 226-235. doi: 10.1007/s40846-016-0120-5
11. Liang Y, Lee D, Li Y, et al. Unpaired medical image colorization using generative adversarial network. Multimedia Tools and Applications. 2021; 81(19): 26669-26683. doi: 10.1007/s11042-020-10468-6
12. Chen S, Xiao N, Shi X, et al. ColorMedGAN: A Semantic Colorization Framework for Medical Images. Applied Sciences. 2023; 13(5): 3168. doi: 10.3390/app13053168
13. Ronneberger O, Fischer P, Brox T. U-net: Convolutional networks for biomedical image segmentation. In: Navab N, Hornegger J, Wells W, Frangi A (editors). *Medical Image Computing and Computer-Assisted Intervention—MICCAI 2015*, Proceedings of 18th International Conference; 5–9 October 2015; Munich, Germany. Springer, Cham; 2017. pp. 234–241. doi: 10.1007/978-3-319-24574-4_28
14. Kiani L, Saeed M, Nezamabadi-pour H. Image colorization using generative adversarial networks and transfer learning. In: Proceedings of 2020 International Conference on Machine Vision and Image Processing (MVIP); 18–20 February 2020; Iran. pp. 1–6. doi: 10.1109/MVIP49855.2020.9116882
15. Coyle EJ, Lin JH. Stack filters and the mean absolute error criterion. IEEE Transactions on Acoustics, Speech, and Signal Processing. 1988; 36(8): 1244-1254. doi: 10.1109/29.1653
16. Wang Z, Bovik AC, Sheikh HR, et al. Image Quality Assessment: From Error Visibility to Structural Similarity. IEEE Transactions on Image Processing. 2004; 13(4): 600-612. doi: 10.1109/tip.2003.819861
17. HuBMAP Hacking the Kidney. Available online: http://Kaggle.com/c/hubmap-kidney-segmentation (accessed on 22 December 2023).